LC-TH-2000-058

Februrary 2001

Search for Extra Dimensions in Graviton Emission $e^+e^- \longrightarrow \gamma G$

Anja Vest

I. Physikalisches Institut der RWTH, D-52056 Aachen, Germany

Abstract

The possibility of discovering direct graviton production in the process $e^+e^- \to \gamma G$ at the TESLA linear collider is calculated for an integrated luminosity of 500 fb^{-1} at $\sqrt{s} = 500$ GeV and for 1000 fb^{-1} at $\sqrt{s} = 800$ GeV. The aim of this analysis is the determination of the exclusion limits of the mass scale M_D dependent on the number of extra dimensions δ for a confidence level of 95 %. The signature is a single photon and missing energy. Therefore the major Standard Model background is the neutrino production $e^+e^- \to \nu\bar{\nu}\gamma$. The study of the signal and the backround is done by Monte Carlo simulation programs including beamstrahlung and initial state radiation. Polarisation of the electron and positron beams is also considered which leads to a better signal to background ratio. The simulation of the events is done with the help of the full detector simulation SIMDET.

1 Introduction

1.1 The hierachy-problem

In nature there are three fundamental energy scales:

- the electroweak scale,

$$m_{EW} = \frac{1}{(G_F\sqrt{2})^{\frac{1}{2}}} \approx 246\,\mathrm{GeV},$$

- the infrared cut-off-parameter of the QCD,

$$\Lambda_{QCD} \approx 200\,\mathrm{MeV},$$

- and the Planck scale

$$M_P = \frac{1}{\sqrt{G_N}} = 1.2 \cdot 10^{19}\,\mathrm{GeV},$$

At the Planck scale gravity becomes as strong as the electroweak interaction. The difference between the magnitudes of the energy scales is called hierachy. m_{EW} and Λ_{QCD} are very close compared to the Planck scale ($\frac{m_{EW}}{M_P} \approx 2 \cdot 10^{-17}$). So far the origin of the hierachy problem could not be solved.

One important difference between the scales Λ_{QCD}, m_{EW} and M_P is that the strong and the electroweak interactions have been probed at distances $\sim \frac{1}{m_{EW}}$, while the gravitational forces have only been probed at distances of about 1 mm. At energies $\sim M_P$ it is not possible to measure gravity in classical experiments. At distances $\sim \frac{1}{M_P}$ there will be quantum-effects which require a transition from gravity to quantum-gravity.

The physics of the electroweak scale m_{EW} is well tested by experiments. For many theorists a close spacing of all fundamental scales seems very desirable. Therefore Arkani-Hamed, Dimopoulos and Dvali (ADD) [AHDD98] suggested that gravity becomes strong at a scale $M_D \sim 1$ TeV. They explained the weakness of gravity at low energies by the presence of δ extra dimensions of 'radius' R. The scale M_D is the effective Planck mass of this $(4+\delta)$-dimensional theory. So M_D is now of the same magnitude as m_{EW}.

According to the ADD-theory two testmasses m_1 and m_2 placed within a distance $r \ll R$ feel a gravitational potential

$$V(r) \sim \frac{m_1 m_2}{M_D^{\delta+2}} \frac{1}{r^{\delta+1}}, \qquad (r \ll R).$$

If the masses are placed at a distance $r \gg R$ gravity cannot extend in the extra dimensions and the masses feel the usual $\frac{1}{r}$-potential

$$V(r) \sim \frac{m_1 m_2}{M_D^{\delta+2} R^\delta} \frac{1}{r}, \qquad (r \gg R)$$

Therefore the effective 4-dimensional Planck can be expressed by

$$\frac{1}{G_N} = M_P^2 \sim R^\delta M_D^{\delta+2} \tag{1}$$

Supposing $M_D \sim m_{EW}$ and demanding that R is chosen to reproduce the observed Planck mass one gets:

$$R \approx 10^{\frac{32}{\delta}-19}\,\mathrm{m}.$$

Modifications of Newton's law of gravity will be noticable only at distances smaller than R [GRW98].

For $\delta = 1$ one gets $R \approx 10^{13}$ m, so this case is empirically excluded. The case $\delta = 2$ leads to $R \approx 1$ mm. For all $\delta > 2$ gravity cannot be measured and equation 1 is consistent with already existing experiments.

1.2 Kaluza-Klein-excitations

The basic assumption of the ADD-model is that the only fields which can propagate in the $4+\delta$-dimensional space are the gravitons. The graviton states can be characterised by a quantified momentum within the extra dimensions. The states with a momentum $\neq 0$ are called Kaluza-Klein(KK)-states. These graviton KK-modes have masses $\sim \frac{|n|}{R}$ where n is the quantum-number of the modes. Therfore the different KK-states have mass-splittings [GRW98]

$$\Delta m \sim \frac{1}{R}.$$

Here the relation between the gravitational constant G_N and the scale M_D (equation 1) was used.

In four dimensions the KK-modes can be described as massive spin-2 states. These states correspond to the gravitons G and couple with the strength M_P^{-1} to SM particles.

Summation over all KK-states leads to a coupling $\sim M_D^4$ which means that gravity becomes strong at a scale $M_D \ll M_P$.

1.3 Collider-experiments

If the mass scale of quantum-gravity is low, i.e. if gravity becomes strong at energies ~ 1 TeV the observation of graviton radiation could be possible in collider-experiments.

In e^+e^--collisions at a linear collider the process

$$e^+e^- \longrightarrow \gamma G$$

is the source of graviton radiation and it is analysed here.

In high energy particle collisions gravitons should be produced at significant rates. Following the ADD-theory a graviton is a neutral, massive non-interacting spin-2 particle wich cannot be seen by a collider detector. Therefore graviton radiation leads to signatures with a single photon and missing transverse energy:

$$e^+e^- \longrightarrow \gamma + E_T^{miss}.$$

The Feynman-diagram is shown in figure 1.

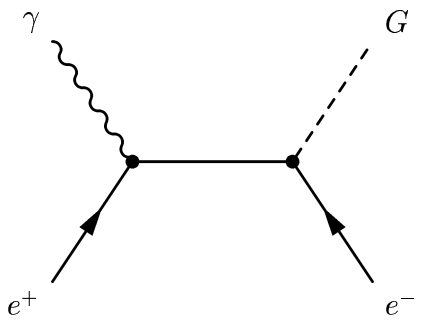

Figure 1: Feynman-diagram of the direct graviton production in e^+e^--collisions

2 The cross-section

If δ is not too large, the mass-splitting Δm is very small. Therefore the sum over all KK-states can now be written as an integral.

The differential cross-section is given by [GRW98]:

$$\frac{d^2\sigma_G}{dx_\gamma d\cos\theta_\gamma} = \frac{\alpha}{64} S_{\delta-1} \left(\frac{\sqrt{\hat{s}}}{M_D}\right)^{\delta+2} \frac{1}{\hat{s}} f(x_\gamma, \cos\theta_\gamma) \tag{2}$$

with

$$f(x,y) = \frac{2(1-x)^{\frac{\delta}{2}-1}}{x(1-y^2)}\Big((2-x)^2(1-x+x^2) - 3y^2x^2(1-x) - y^4x^4\Big)$$

$\sqrt{\hat{s}}$ is the center of mass energy after ISR which is calculated by:

$$\sqrt{\hat{s}} = \sqrt{\left(p'_{e^+} + p'_{e^-}\right)^2}.$$

Here p'_{e^+} and p'_{e^-} are the momentum four vectors of the electrons and positrons after ISR.

$x_\gamma = \frac{2E_\gamma}{\sqrt{\hat{s}}}$ ist the photon-energy fraction and $S_{\delta-1}$ is the surface area of a δ-dimensional sphere of unit radius. Though the graviton production in electron-positron-collisions is a two-body-process the differential cross-section depends on two variables because of the continuous distribution of the graviton-mass:

$$m = \sqrt{\hat{s}(1-x_\gamma)}.$$

3 The generator

The cross-section includes Beamstrahlung which is calculated by the program CIRCE [Ohl96].

Besides including ISR the differential-cross section is given by:

$$\frac{d\sigma}{dz_1 dz_2 d\cos\theta_1 d\cos\theta_2 d\cos\theta_\gamma dx_\gamma} = \frac{d^2\sigma_G}{d\cos\theta_\gamma dx_\gamma} f_{e/e,1} f_{e/e,2} f_{\theta_1} f_{\theta_2}$$

where $f_{e/e,1}$, $f_{e/e,2}$, f_{θ_1} and f_{θ_2} are distribution-functions of the energy and the polar-angle of the ISR-Photons. The distribiution-functions of the energies of the ISR-photons are given by [Ber]:

$$f_{e/e,i} = \frac{\alpha}{2\pi} P_{e/e,i} L$$

with the splitting function

$$P_{e/e,i} = \frac{1+z_i^2}{1-z_i}.$$

α is the running coupling-constant of QED and L is a model dependent logarithmic factor which has been set to

$$L = \ln\left(\frac{s}{m_e^2}\right) - \frac{1}{2}.$$

At $\sqrt{s} = 500$ GeV L is ≈ 27.

Because the integrals over $f_{e/e,i}(z)$ from 0 to 1 diverge the integration is divided into two parts by a cut-off-parameter ϵ. Normalisation gives:

$$\int_0^{1-\epsilon} f_{e/e,i}(z_i)dz_i + \int_{1-\epsilon}^{1} k dz_i = 1$$

So one gets:

$$f'_{e/e,i} = \begin{cases} f_{e/e,i} & , z_i < 1-\epsilon \\ \\ k = \frac{1}{\epsilon} - \frac{\alpha}{2\pi\epsilon} L \left(-\frac{3}{2} + 2\epsilon + 2\ln\frac{1}{\epsilon}\right) & , 1-\epsilon < z_i < 1 \end{cases}$$

This prescription represents an adaption of the subscription method used in analytical calculations [Ber]. The distribution-functions of the polar angles of the ISR-photons are given by:

$$f_{\theta_i} = \frac{\sin^2\theta_{\gamma,i}}{(1-\beta\cos\theta_{\gamma,i})^2} N$$

where β is the velocity of the electrons and N is a normalisation-factor. The total cross-section is calculated using the adaptive Monte Carlo simulation BASES [Kaw95].

4 The Standard Model background

The signature of the graviton-production is a single photon with high p_T and missing energy. So the major standardmodel-background is [Tre89]:

$$e^+e^- \longrightarrow \nu\bar{\nu}\gamma$$

The feynman-diagrams are shown in figure 2.

In table 1 the calculated unpolarised cross-sections for the signal and the background at different center of mass energies are shown.

E_{CMS}	σ_S in pb	σ_B in pb
$\sqrt{s} = 500$ GeV	5.31	3.79
$\sqrt{s} = 800$ GeV	17.61	4.24

Table 1: unpolarised cross-sections of the signal ($M_D = 1$ TeV and $\delta = 2$) and the background

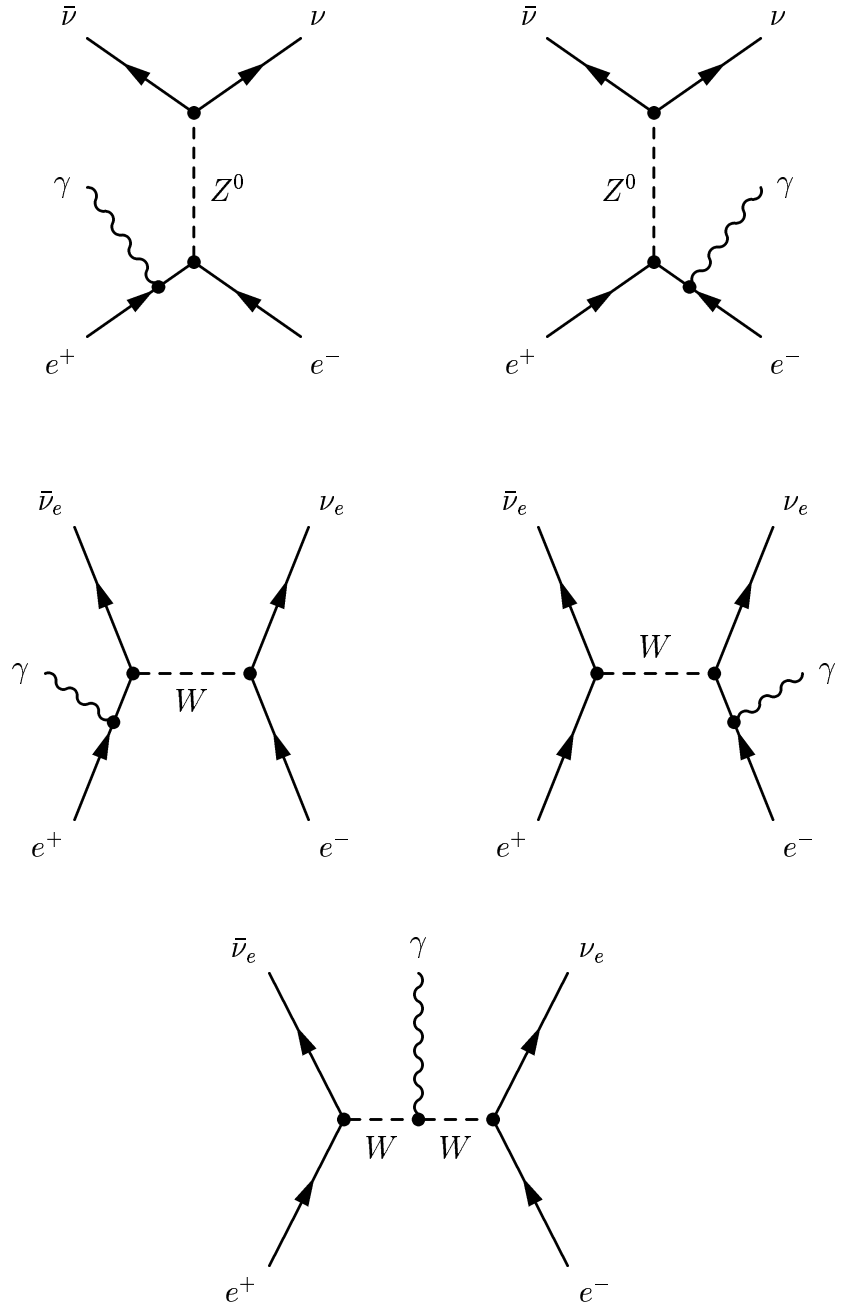

Figure 2: Feynman-diagrams of the SM-background $e^+e^- \longrightarrow \nu\bar{\nu}\gamma$

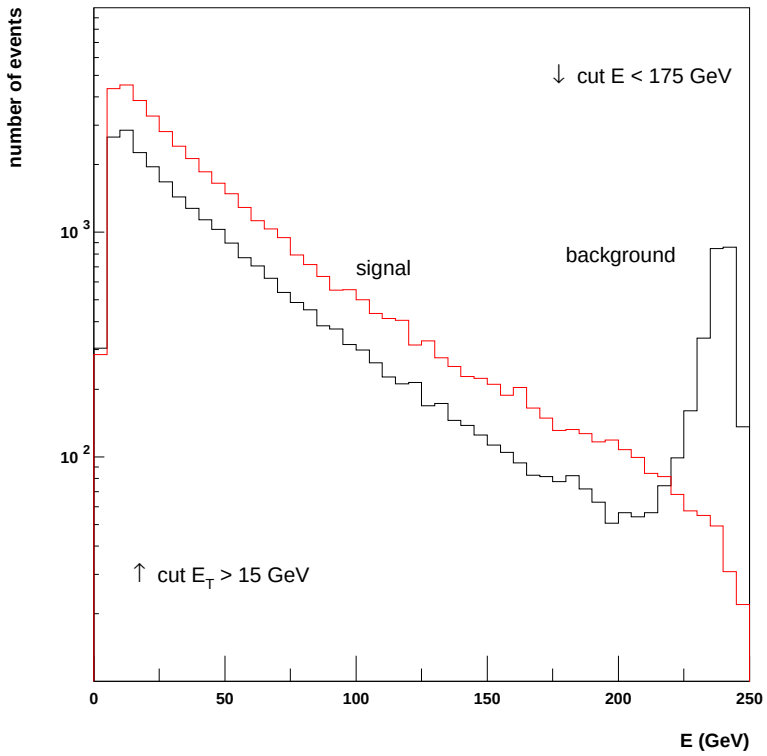

Figure 3: Spectrum of the SM-background $e^+e^- \to \nu\bar{\nu}\gamma$ at $\sqrt{s} = 500$ GeV. The signal-spectrum is also shown for $\delta = 2$ and $M_D = 2$ TeV.

5 Kinematic cuts

The following kinematic acceptance cuts are imposed on the photon:

- Within the ECAL acceptance: $\sin\theta_\gamma > 0.1$.
- $p_T > 0.06 E_{beam}$ in order to reject events with no genuine missing p_T such as the Bhabha-scattering $e^+e^- \to e^+e^-\gamma$ where electrons at polar angles below the ECAL acceptance mimic missing p_T.
- $E_\gamma < 175$ GeV at $\sqrt{s} = 500$ GeV and $E_\gamma < 250$ GeV at $\sqrt{s} = 800$ GeV in order to reject the energetic photons from the standardmodel-background which arise from $e^+e^- \to Z^0\gamma$.

6 Polarisation

The contribution of $e^+e^- \longrightarrow Z^0\gamma$ to the SM-background is eliminated by the upper cut in E_γ. So only the contribution of the W-exchange remains. Because of helicity-conservation

the background-reaction is only existing for left-handed electrons and right-handed positrons:

$$e^+_R e^-_L \longrightarrow \nu_{e,L}\bar{\nu}_{e,R}\gamma$$

Therefore polarised electron and positron beams are extremely effective in suppressing the SM-background. Besides using polarised beams the signal-cross-section can be improved. A polarisation of $P_{e^-_R} = 0.8$ for the electrons and $P_{e^+_L} = -0.6$ for the positrons might be possible. With polarisation it is possible to extend the reach of a linear collider in the quest for evidence of extra-dimensions. Table 2 shows how polarisation can improve the signal to background ratio.

$P_{e^-_R} = 0$ $P_{e^+_L} = 0$	$\sigma_{pol,S} = \sigma_{0,S}$	$\sigma_{pol,B} = \sigma_{0,B}$	$\frac{\sigma_{pol,S}}{\sigma_{pol,B}} = \frac{\sigma_{0,S}}{\sigma_{0,B}}$
$P_{e^-_R} = 0.8$ $P_{e^+_L} = 0$	$\sigma_{pol,S} = \sigma_{0,S}$	$\sigma_{pol,B} = 0.2\sigma_{0,B}$	$\frac{\sigma_{pol,S}}{\sigma_{pol,B}} = 5\frac{\sigma_{0,S}}{\sigma_{0,B}}$
$P_{e^-_R} = 0.8$ $P_{e^+_L} = -0.45$	$\sigma_{pol,S} = 1.36\sigma_{0,S}$	$\sigma_{pol,B} = 0.11\sigma_{0,B}$	$\frac{\sigma_{pol,S}}{\sigma_{pol,B}} = 12.36\frac{\sigma_{0,S}}{\sigma_{0,B}}$
$P_{e^-_R} = 0.8$ $P_{e^+_L} = -0.6$	$\sigma_{pol,S} = 1.48\sigma_{0,S}$	$\sigma_{pol,B} = 0.08\sigma_{0,B}$	$\frac{\sigma_{pol,S}}{\sigma_{pol,B}} = 18.5\frac{\sigma_{0,S}}{\sigma_{0,B}}$

Table 2: Influence of the polarisation on the cross-sections

7 Determination of the exclusion limit of the mass scale M_D

The process of direct graviton production $e^+e^- \longrightarrow \gamma G$ is calculated for an integrated luminosity of $L_{int} = 500$ fb^{-1} at $\sqrt{s} = 500$ GeV and for $L_{int} = 1000$ fb^{-1} at $\sqrt{s} = 800$ GeV. The exclusion limit of the mass scale M_D is calculated for CL = 95 %. The number of the selected events is given by:

$$N = \epsilon\, \sigma L_{int}$$

where ϵ is the efficiency of selecting N events.

To analyse the process $e^+e^- \longrightarrow \gamma G$ the spectra of the transverse photon energy $E_{T,\gamma}$ of the signal and the background are compared by the χ^2-test. For this analysis the following parameters are used:

- $L_{int} = 500\,\text{fb}^{-1}$ at $\sqrt{s} = 500\,\text{GeV}$
- $L_{int} = 1000\,\text{fb}^{-1}$ at $\sqrt{s} = 800\,\text{GeV}$

- $P_{e_R^-} = 0, 0.8$
- $P_{e_L^+} = 0, -0.45, -0.6$
- $\delta = 2, 3, 4, 5, 6, 7$
- $1 < M_D < 12.5\,\text{TeV}$ in steps of 0.25 TeV or 0.5 TeV

The simulation of the events is done with the help of the full detector simulation SIMDET [SP] which is based on a description of a liner collider detector in the TESLA-CDR [CDR97].

7.1 The χ^2-test

The spectra of the transverse photon energies are displayed in histograms with n bins, where the binwidth is chosen to represent the energy resolution of the ECAL. At $\sqrt{s} = 500$ GeV the binwidth is 2.5 GeV and at $\sqrt{s} = 800$ GeV the binwidth is 4 GeV.

Adapting the method of the H1-collaboration [Col00] the χ^2-function is defined as ([Bra99]):

$$\chi^2 = \sum_{i=1}^{n} \frac{(N_{exp,i} - N_{th,i})^2}{N_{exp,i}},$$

The variation of the parameter M_D changes the χ^2 value by a certain amount to the SM fit:

$$\Delta\chi^2 = \chi^2_{SM+G} - \chi^2_{SM}$$

Taking into account the dominant error source and uncertanties $\Delta\chi^2$ is given by:

$$\Delta\chi^2 = \sum_{i=1}^{n} \frac{(N_{B+S,i} - f_N N_{B,i})^2}{f_N^2 N_{B,i}} + \left(\frac{1 - f_N}{\Delta f_N}\right)^2,$$

with $N_{B+S,i} = N_{B,i} + N_{S,i}$. Here f_N is an overall normalisation parameter with an uncertainty $\Delta f_N = 0.01$ or $\Delta f_N = 0.001$. The parameter f_N can be found by calculating the minimum of the $\Delta\chi^2$-distribution. The 95 % confidence level of the χ^2-distribution with one degree of freedom is given by $\chi^2 < 3.84$. We have chosen $\Delta\chi^2 = 3.84$ although a onesided test allows for $\Delta\chi^2 = 2.56$ yielding even better limits.

7.2 Results

Examples of the influence of polarisation, of the mass scale M_D and of the number of extra dimensions δ on the spectra of the transverse photon energy of the signal and the background at $\sqrt{s} = 500$ GeV are shown in the figures 6 to 8.

Because for all $\delta \geq 2$ a certain M_D at 95 % CL ($\Delta\chi^2 = 3.84$) is connected with one certain cross-section it is possible to illustrate the exclusion limits of the mass scale M_D by

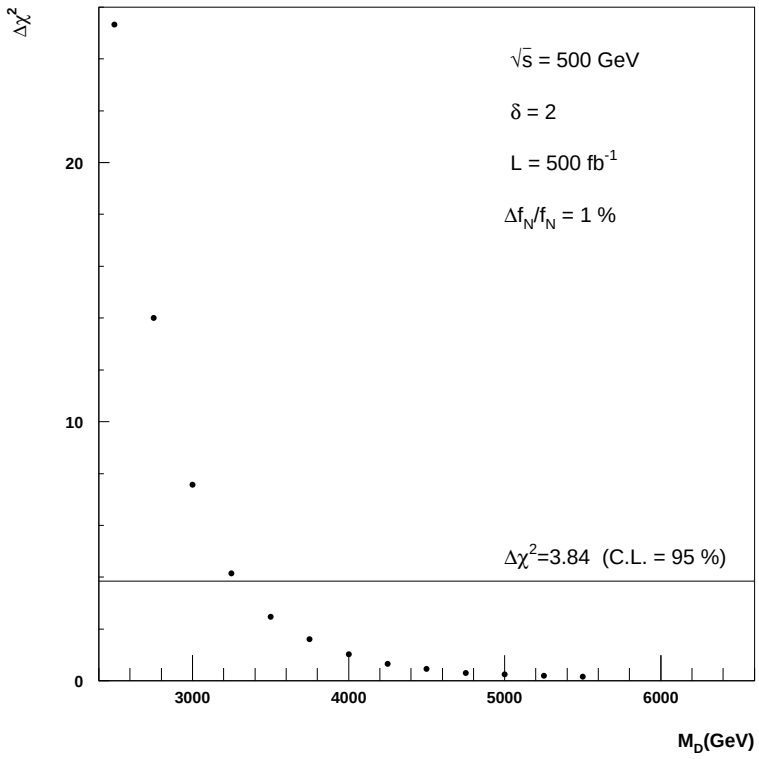

Figure 4: Distribution of $\Delta\chi^2$ dependent on the mass scale M_D for $\delta = 2$ at $\sqrt{s} = 500\,\mathrm{GeV}$ ($L_{int} = 500\,\mathrm{fb}^{-1}$) and $\frac{\Delta f_N}{f_N} = 1\,\%$. The horizontal line illustrates the exlusion limit of M_D for CL = 95 %, i.e. $\Delta\chi^2 = 3.84$.

a horizontal line in a plot σ vs. M_D. The figuers 9 and 10 show the total cross-section of the direct graviton production in e^+e^--collisions dependent on the mass scale M_D. The horizontal lines illustrate the cross-section at a 95 % CL on the exclusion limit of the mass scale for $\frac{\Delta f_N}{f_N} = 1\,\%$ and $\frac{\Delta f_N}{f_N} = 0.1\,\%$. These cross-sections are shown without polarisation in figure 9 and with polarisation $P_{e_R^-} = 0.8$ and $P_{e_L^+} = -0.45$ in figure 10.

In the tables 4 and 5 all exclusion limits of the mass scale M_D dependent on the polarisation, δ and $\frac{\Delta f_N}{f_N}$ are summarised. For $\delta = 2$ an exclusion limit for the mass scale of 10.9 TeV can be reached.

At $\sqrt{s} = 800$ GeV for $M_D = 7.5$ TeV and $\delta = 2$ the cross-section of the signal is calculated to be $\sigma = 1.87$ fb which can also be seen in figure 10.

The discovery limit of 5σ, i.e. $\Delta\chi^2 = 25$, for direct graviton production is illustrated by the dashed lines for $\frac{\Delta f_N}{f_N} = 0.1\,\%$ without polarisation in figure 9 and with $P_{e_R^-} = 0.8$ and $P_{e_L^+} = -0.45$ in figure 10.

7.3 Determination of the error of the mass scale

If at the NLC the direct graviton production can be discovered and if the cross-sections will be measured at two different CMS-energies it will be possible to determine an error of the exclusion limit of the mass scale M_D. The procedure is explained by an example:

If at $\sqrt{s} = 500$ GeV a total cross-section of $\sigma = 0.01$ is measured with an accuracy of 10 %, i.e. $0.09\,\text{pb} < \sigma < 0.11\,\text{pb}$, one can determine a range of the mass scale M_D with the help of figure 9. For $\delta = 3$ one finds $M_D = 2.9^{+0.03}_{-0.07}$ TeV. For this mass range at $\delta = 3$ in figure 10 one can find the corresponding cross-section at $\sqrt{s} = 800$ GeV, which is $\sigma = 0.04^{+0.003}_{-0.005}$ pb. These cross-sections now give the mass ranges for all the other δ.

Now in a plot M_D vs. δ the points which are found by the procedure described above are fitted by a straight line. So a rhomb is produced which gives an error for the exclusion limit of the mass scale.

In figure 5 a plot M_D vs. δ is shown where at $\sqrt{s} = 500$ GeV the cross-section is assumed to be $\sigma = 0.01 \pm 0.001$ pb The mass range is given for $\delta = 3$. So at $\sqrt{s} = 800$ GeV one finds $M_D = 2.9^{+0.03}_{-0.07}$ TeV. The outermost points of the rhomb give the error for the exclusion limit of the mass scale:

$$2.30\,\text{TeV} \;<\; M_D \;<\; 3.15\,\text{TeV}.$$

In table 3 the different errors for the exclusion limit of the mass scale ($\sigma = 0.01 \pm 0.001$ pb at $\sqrt{s} = 500$ GeV) are summarised.

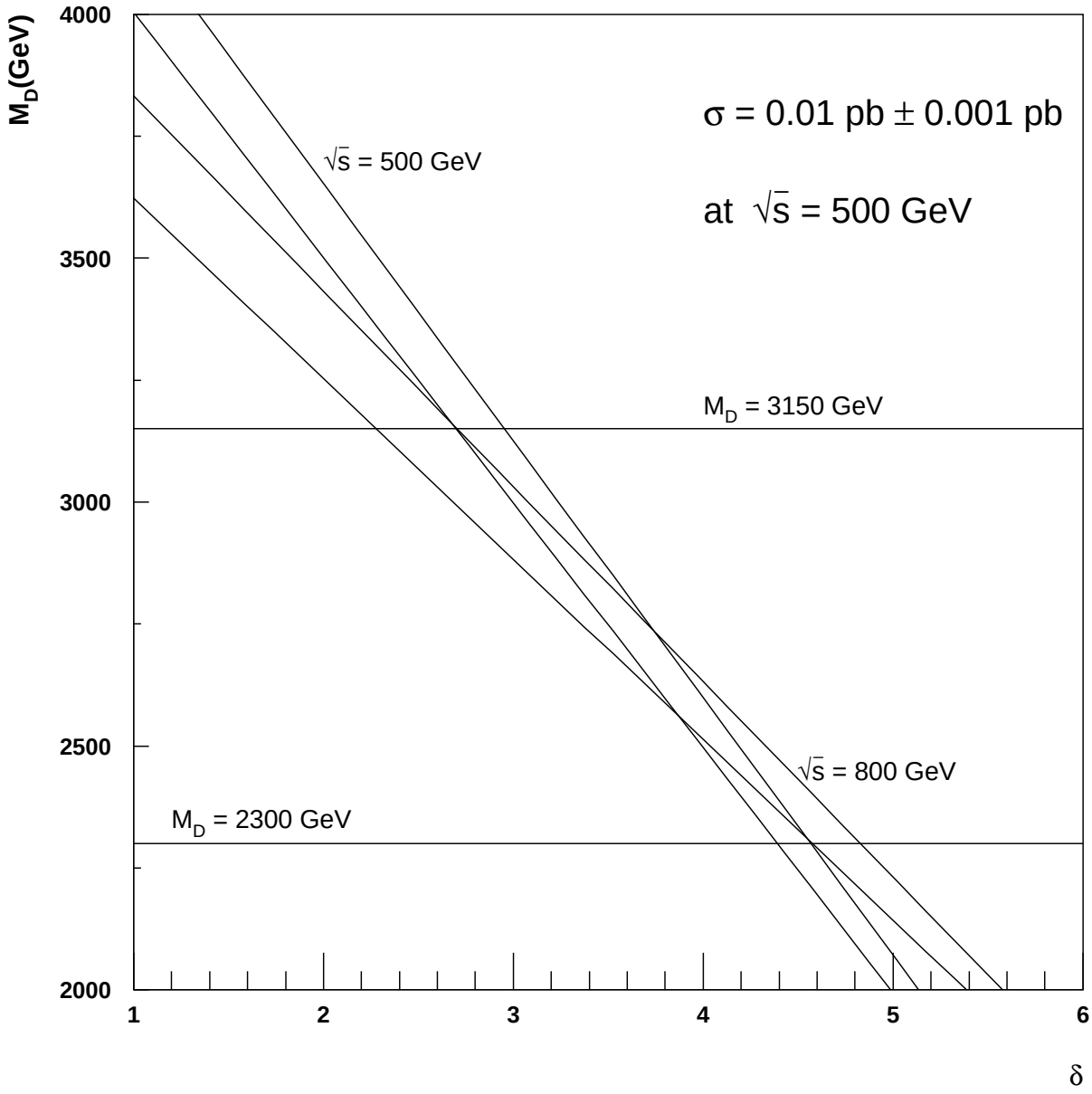

Figure 5: The exclusion limit of the mass scale M_D dependent on the number of extra dimensions δ. Here the mass range is given by a cross-section $\sigma = 0.01 \pm 0.001$ pb at $\sqrt{s} = 500$ GeV and $\delta = 3$.

δ at $\sqrt{s} = 500$ GeV	error of M_D in TeV
$\delta = 2$	$M_D \geq 3.63$
$\delta = 3$	$2.30 < M_D < 3.15$
$\delta = 4$	$1.90 < M_D < 2.25$
$\delta = 5$	$1.64 < M_D < 1.86$
$\delta = 6$	$1.45 < M_D < 1.61$
$\delta = 7$	$1.37 < M_D < 1.47$

Table 3: The errors for the exclusion limit of the mass scale ($\sigma = 0.01 \pm 0.001$ pb at $\sqrt{s} = 500$ GeV)

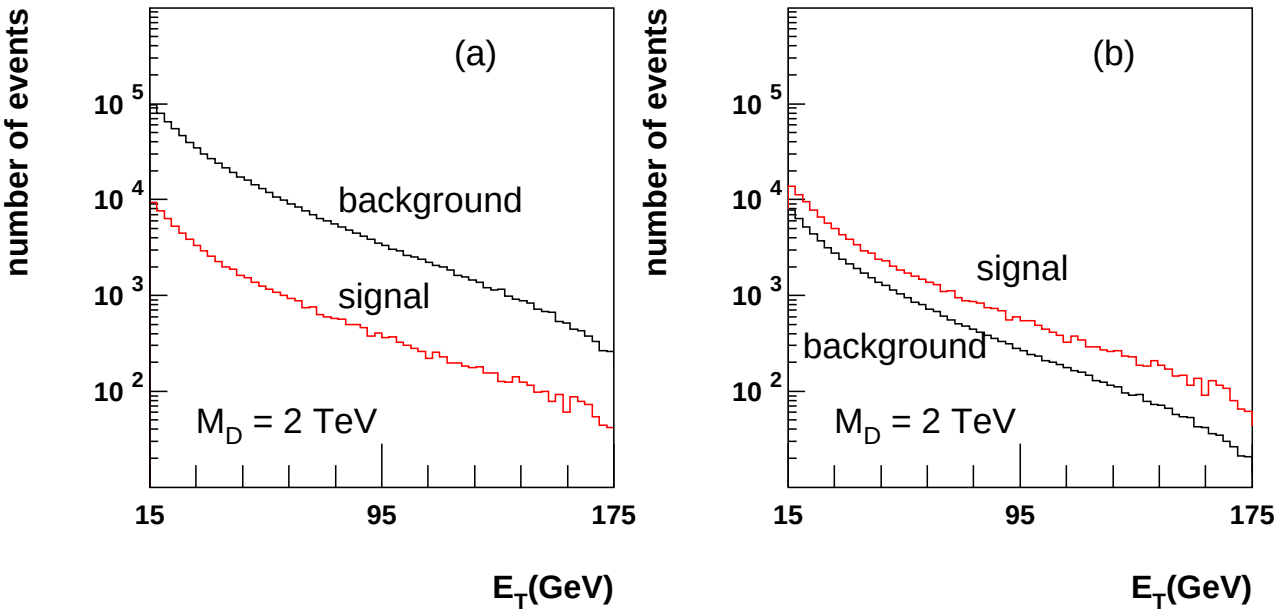

Figure 6: Influence of polarisation on the spectra of the transverse photon energy of the signal and the background at $\sqrt{s} = 500$ GeV ($L_{int} = 500\,\mathrm{fb}^{-1}$). (a) spectra without polarisation, (b) spectra with polarisation $P_{e_R^-} = 0.8$ and $P_{e_L^+} = -0.6$. $M_D = 2\,\mathrm{TeV}$, $\delta = 2$.

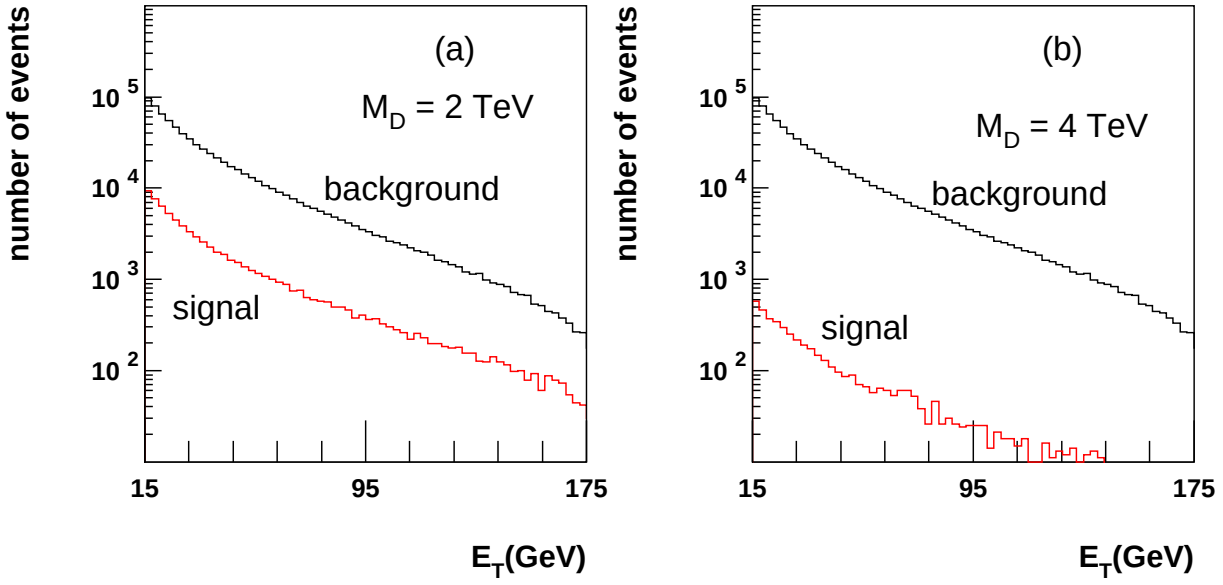

Figure 7: Influence of the mass scale M_D on the spectra of the transverse photon energy of the signal and the background at $\sqrt{s} = 500$ GeV ($L_{int} = 500\,\mathrm{fb}^{-1}$). $\delta = 2$. (a): $M_D = 2\,\mathrm{TeV}$, (b): $M_D = 4\,\mathrm{TeV}$. The underground-spectrum is shown without polarisation.

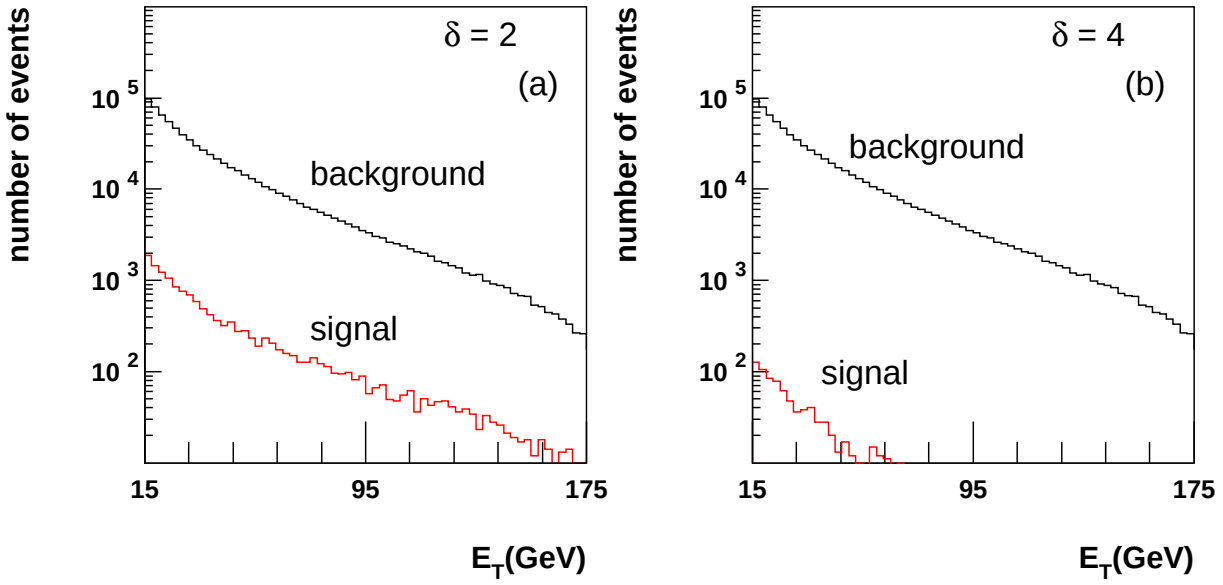

Figure 8: Influence of the number of extra dimensions δ on the spectra of the transverse photon energy of the signal and the background at $\sqrt{s} = 500$ GeV ($L_{int} = 500\,\mathrm{fb}^{-1}$). $M_D = 3\,\mathrm{TeV}$. (a): $\delta = 2$, (b): $\delta = 4$. The underground-spectrum is shown without polarisation.

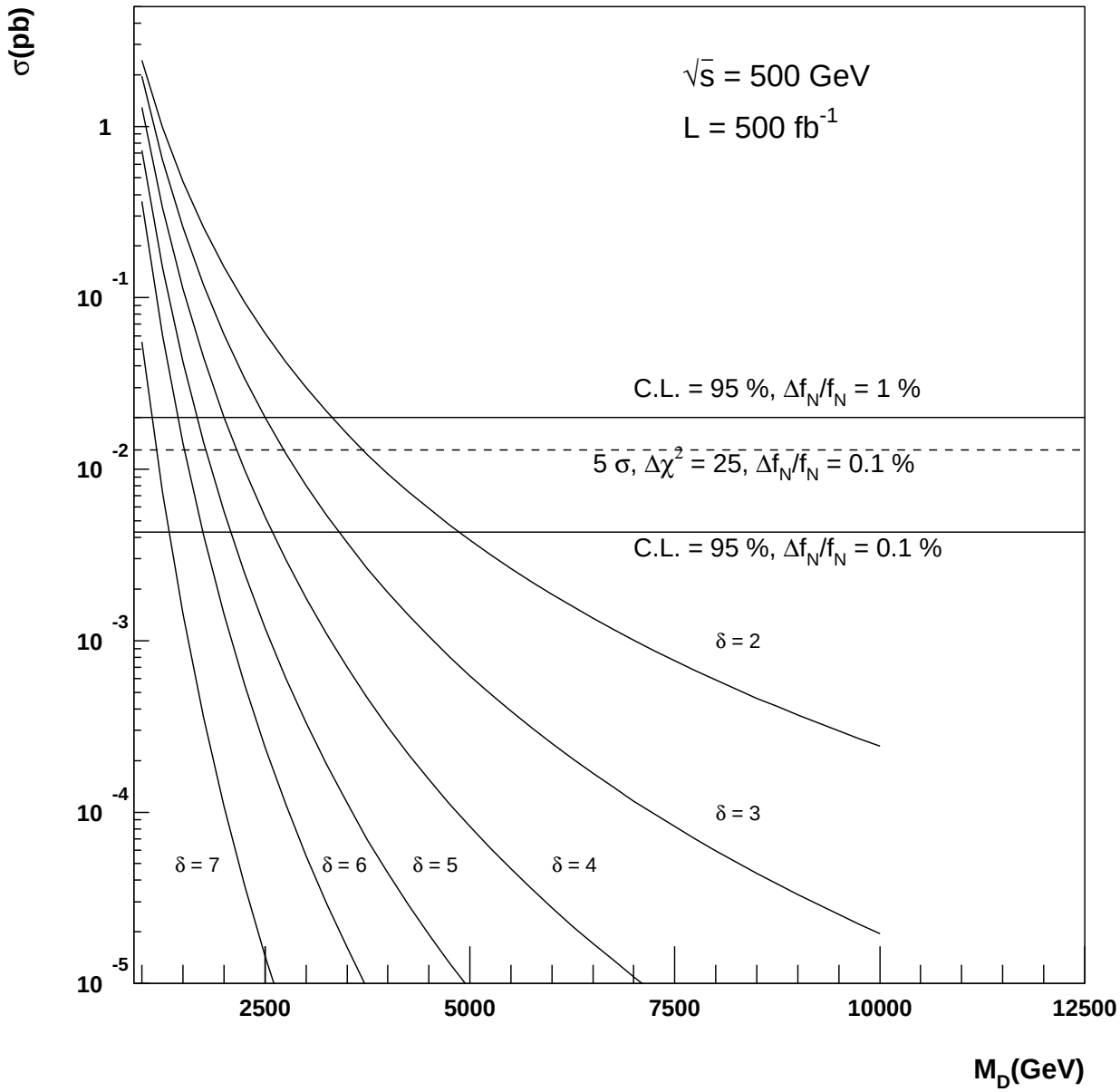

Figure 9: The total cross-section for the graviton production process $e^+e^- \to \gamma G$ at $\sqrt{s} = 500$ GeV ($L_{int} = 500\,\mathrm{fb}^{-1}$) dependent on the mass scale M_D and on the number of extra dimensions δ. The horizontal lines illustrate the exclusion limit of the mass scale M_D for CL = 95 % at $\frac{\Delta f_N}{f_N} = 1\,\%$ and $\frac{\Delta f_N}{f_N} = 0.1\,\%$ without polarisation. The dashed line shows the discovery limit of 5σ, i.e. $\Delta\chi^2 = 25$.

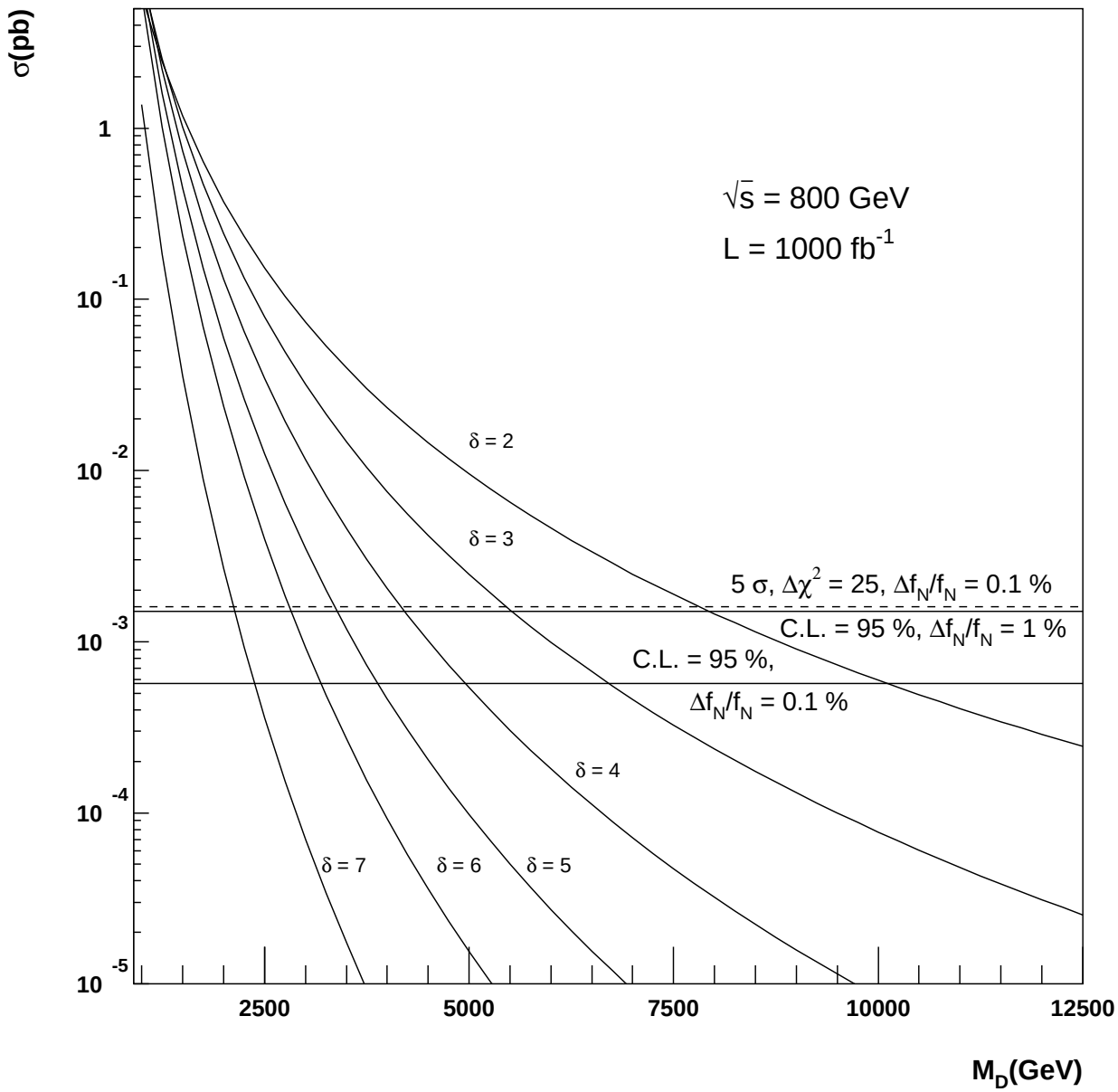

Figure 10: The total cross-section for the graviton production process $e^+e^- \to \gamma G$ at $\sqrt{s} = 800$ GeV ($L_{int} = 1000\,\mathrm{fb}^{-1}$) dependent on the mass scale M_D and on the number of extra dimensions δ. The horizontal lines illustrate the exclusion limit of the mass scale M_D for CL = 95 % at $\frac{\Delta f_N}{f_N} = 1\,\%$ and $\frac{\Delta f_N}{f_N} = 0.1\,\%$ with polarization $P_{e_R^-} = 0.8$ and $P_{e_L^+} = -0.45$. The dashed line shows the discovery limit of 5σ, i.e. $\Delta\chi^2 = 25$.

number of extra dimensions	polarisation	M_D in TeV for C.L.= 95 % at $\frac{\Delta f_N}{f_N} = 1\,\%$	M_D in TeV for C.L.= 95 % at $\frac{\Delta f_N}{f_N} = 0.1\,\%$
$\delta = 2$	$P_{e_R^-} = 0,\ P_{e_L^+} = 0$	3.3	4.8
	$P_{e_R^-} = 0.8,\ P_{e_L^+} = 0$	4.7	6.3
	$P_{e_R^-} = 0.8,\ P_{e_L^+} = -0.45$	5.8	7.4
	$P_{e_R^-} = 0.8,\ P_{e_L^+} = -0.6$	6.3	7.9
$\delta = 3$	$P_{e_R^-} = 0,\ P_{e_L^+} = 0$	2.5	3.4
	$P_{e_R^-} = 0.8,\ P_{e_L^+} = 0$	2.8	4.2
	$P_{e_R^-} = 0.8,\ P_{e_L^+} = -0.45$	4.3	4.8
	$P_{e_R^-} = 0.8,\ P_{e_L^+} = -0.6$	4.6	5.1
$\delta = 4$	$P_{e_R^-} = 0,\ P_{e_L^+} = 0$	2.0	2.7
	$P_{e_R^-} = 0.8,\ P_{e_L^+} = 0$	2.2	3.1
	$P_{e_R^-} = 0.8,\ P_{e_L^+} = -0.45$	2.7	3.4
	$P_{e_R^-} = 0.8,\ P_{e_L^+} = -0.6$	2.8	3.6
$\delta = 5$	$P_{e_R^-} = 0,\ P_{e_L^+} = 0$	1.7	2.2
	$P_{e_R^-} = 0.8,\ P_{e_L^+} = 0$	1.9	2.4
	$P_{e_R^-} = 0.8,\ P_{e_L^+} = -0.45$	2.5	2.7
	$P_{e_R^-} = 0.8,\ P_{e_L^+} = -0.6$	2.6	2.8
$\delta = 6$	$P_{e_R^-} = 0,\ P_{e_L^+} = 0$	1.4	1.7
	$P_{e_R^-} = 0.8,\ P_{e_L^+} = 0$	1.6	2.0
	$P_{e_R^-} = 0.8,\ P_{e_L^+} = -0.45$	2.0	2.2
	$P_{e_R^-} = 0.8,\ P_{e_L^+} = -0.6$	2.1	2.3
$\delta = 7$	$P_{e_R^-} = 0,\ P_{e_L^+} = 0$	1.1	1.3
	$P_{e_R^-} = 0.8,\ P_{e_L^+} = 0$	1.2	1.5
	$P_{e_R^-} = 0.8,\ P_{e_L^+} = -0.45$	1.5	1.6
	$P_{e_R^-} = 0.8,\ P_{e_L^+} = -0.6$	1.6	1.7

Table 4: The exclusion limits of M_D in TeV dependent on the polarisation, δ and $\frac{\Delta f_N}{f_N}$ at $\sqrt{s} = 500\,\text{GeV}$ ($L_{int} = 500\,\text{fb}^{-1}$) for CL = 95 %.

number of extra dimensions	polarisation	M_D in TeV for C.L.= 95 % at $\frac{\Delta f_N}{f_N} = 1\,\%$	M_D in TeV for C.L.= 95 % at $\frac{\Delta f_N}{f_N} = 0.1\,\%$
$\delta = 2$	$P_{e_R^-} = 0,\ P_{e_L^+} = 0$	4.2	6.4
	$P_{e_R^-} = 0.8,\ P_{e_L^+} = 0$	6.1	8.5
	$P_{e_R^-} = 0.8,\ P_{e_L^+} = -0.45$	7.9	10.2
	$P_{e_R^-} = 0.8,\ P_{e_L^+} = -0.6$	8.4	10.9
$\delta = 3$	$P_{e_R^-} = 0,\ P_{e_L^+} = 0$	3.2	4.7
	$P_{e_R^-} = 0.8,\ P_{e_L^+} = 0$	4.5	5.8
	$P_{e_R^-} = 0.8,\ P_{e_L^+} = -0.45$	5.5	6.7
	$P_{e_R^-} = 0.8,\ P_{e_L^+} = -0.6$	5.8	7.2
$\delta = 4$	$P_{e_R^-} = 0,\ P_{e_L^+} = 0$	2.7	3.6
	$P_{e_R^-} = 0.8,\ P_{e_L^+} = 0$	3.5	4.5
	$P_{e_R^-} = 0.8,\ P_{e_L^+} = -0.45$	4.6	5.0
	$P_{e_R^-} = 0.8,\ P_{e_L^+} = -0.6$	4.3	5.2
$\delta = 5$	$P_{e_R^-} = 0,\ P_{e_L^+} = 0$	2.3	3.0
	$P_{e_R^-} = 0.8,\ P_{e_L^+} = 0$	2.9	3.5
	$P_{e_R^-} = 0.8,\ P_{e_L^+} = -0.45$	3.4	3.9
	$P_{e_R^-} = 0.8,\ P_{e_L^+} = -0.6$	3.5	4.1
$\delta = 6$	$P_{e_R^-} = 0,\ P_{e_L^+} = 0$	2.0	2.5
	$P_{e_R^-} = 0.8,\ P_{e_L^+} = 0$	2.8	3.0
	$P_{e_R^-} = 0.8,\ P_{e_L^+} = -0.45$	2.8	3.2
	$P_{e_R^-} = 0.8,\ P_{e_L^+} = -0.6$	2.9	3.3
$\delta = 7$	$P_{e_R^-} = 0,\ P_{e_L^+} = 0$	1.6	1.9
	$P_{e_R^-} = 0.8,\ P_{e_L^+} = 0$	1.9	2.2
	$P_{e_R^-} = 0.8,\ P_{e_L^+} = -0.45$	2.1	2.3
	$P_{e_R^-} = 0.8,\ P_{e_L^+} = -0.6$	2.2	2.5

Table 5: The exclusion limits of M_D in TeV dependent on the polarisation, δ and $\frac{\Delta f_N}{f_N}$ at $\sqrt{s} = 800\,\text{GeV}$ ($L_{int} = 1000\,\text{fb}^{-1}$) for CL = 95 %.

References

[AHDD98] N. Arkani-Hamed, S. Dimopoulos, and G. Dvali. The Hierachy Problem and New Dimensions at a Millimeter. hep-ph/9803315, March 1998.

[Ber] Ch. Berger. *Elementarteilchenphysik*. In preparation, Springer-Verlag.

[Bra99] S. Brandt. *Datenanalyse. Mit statistischen Methoden und Computerprogrammen.* Spektrum Akademischer Verlag, 1999.

[CDR97] Conceptual Design of a 500 GeV e^+e^- Linear Collider with Integrated X-Ray Laser Facility. DESY 97-048, March 1997.

[Col00] H1 Collaboration. Search for Compositeness, Leptoquarks and Large Extra Dimensions in eq Contact Interactions at HERA. DESY 00-027, February 2000.

[GRW98] G. F. Giudice, R. Ratazzi, and J. D. Wells. Quantum Gravity and Extra Dimension at High-Energy Colliders. hep-ph/9811291, November 1998.

[Kaw95] S. Kawabata. A new version of the multi-dimensional integration and event-generation package BASES/SPRING. *KEK Preprint 94-197, Z. Phys. C*, 62:127, February 1995.

[Ohl96] Thorsten Ohl. CIRCE Version 1.02: Beam Spectra for Simulating Linear Collider Physics. hep-ph/9607454, July 1996.

[SP] H. J. Schreiber and M. Pohl. SIMDET - Version 3. A Parametric Monte Carlo for a TESLA Detector. http://www.ifh.de/linear_collider/users_guide_simdetv301.html.

[Tre89] L. Trentadue. Neutrino Counting. Z-Physics at LEP, CERN 89-08, September 1989.